


ORIGINAL RESEARCH ARTICLE

Traumatic Brain Injury Impairs Systemic Vascular Function through Disruption of Inward-Rectifier Potassium Channels

Adrian M. Sackheim¹, Nuria Villalba¹, Maria Sancho², Osama F. Harraz ²,
Adrian D. Bonev², Angelo D'Alessandro^{3,4}, Travis Nemkov⁴,
Mark T. Nelson^{2,5}, Kalev Freeman^{1,2,*}

¹Department of Surgery, University of Vermont Larner College of Medicine, Burlington, VT, USA, ²Department of Pharmacology, University of Vermont Larner College of Medicine, Burlington, VT, USA, ³Department of Surgery, University of Colorado School of Medicine, Aurora, CO, USA, ⁴Department of Biochemistry and Molecular Genetics, University of Colorado School of Medicine, Aurora, CO, USA, ⁵Division of Cardiovascular Sciences, University of Manchester, Manchester, UK

*Address correspondence to K.F. (e-mail: kalev.freeman@uvm.edu)

Abstract

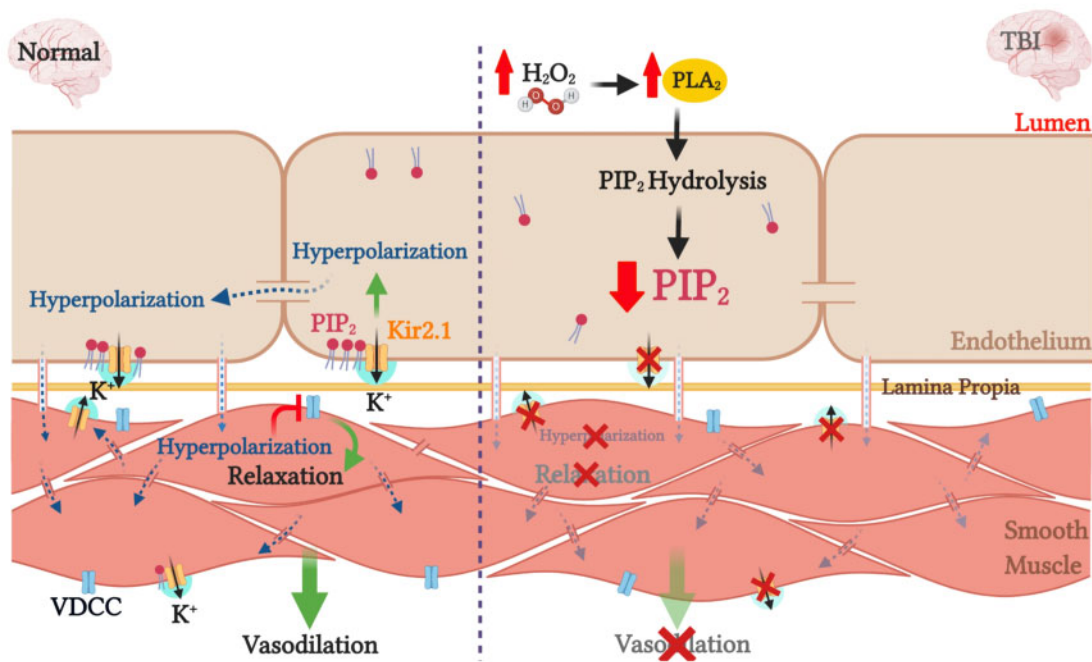
Trauma can lead to widespread vascular dysfunction, but the underlying mechanisms remain largely unknown. Inward-rectifier potassium channels (Kir2.1) play a critical role in the dynamic regulation of regional perfusion and blood flow. Kir2.1 channel activity requires phosphatidylinositol 4,5-bisphosphate (PIP₂), a membrane phospholipid that is degraded by phospholipase A₂ (PLA₂) in conditions of oxidative stress or inflammation. We hypothesized that PLA₂-induced depletion of PIP₂ after trauma impairs Kir2.1 channel function. A fluid percussion injury model of traumatic brain injury (TBI) in rats was used to study mesenteric resistance arteries 24 h after injury. The functional responses of intact arteries were assessed using pressure myography. We analyzed circulating PLA₂, hydrogen peroxide (H₂O₂), and metabolites to identify alterations in signaling pathways associated with PIP₂ in TBI. Electrophysiology analysis of freshly-isolated endothelial and smooth muscle cells revealed a significant reduction of Ba²⁺-sensitive Kir2.1 currents after TBI. Additionally, dilations to elevated extracellular potassium and BaCl₂- or ML 133-induced constrictions in pressurized arteries were significantly decreased following TBI, consistent with an impairment of Kir2.1 channel function. The addition of a PIP₂ analog to the patch pipette successfully rescued endothelial Kir2.1 currents after TBI. Both H₂O₂ and PLA₂ activity were increased after injury. Metabolomics analysis demonstrated altered lipid metabolism signaling pathways, including increased arachidonic acid, and fatty acid mobilization after TBI. Our findings support a model in which increased H₂O₂-induced PLA₂ activity after trauma hydrolyzes endothelial PIP₂, resulting in impaired Kir2.1 channel function.

Submitted: 12 February 2021; Revised: 22 March 2021; Accepted: 23 March 2021

© The Author(s) 2021. Published by Oxford University Press on behalf of American Physiological Society.

This is an Open Access article distributed under the terms of the Creative Commons Attribution Non-Commercial License (<http://creativecommons.org/licenses/by-nc/4.0/>), which permits non-commercial re-use, distribution, and reproduction in any medium, provided the original work is properly cited. For commercial re-use, please contact journals.permissions@oup.com

Graphical Abstract



Key words: traumatic brain injury; vascular endothelium; ion channels; metabolopathy

Introduction

Traumatic injury represents the most common cause of death in individuals under 44 years old, with the majority of these fatalities due to traumatic brain injury (TBI).¹ In addition to the primary mechanical injury, systemic inflammation subsequent to trauma contributes to coagulopathy, vascular leak, and multiorgan dysfunction. Vascular endothelial cells (ECs) are especially vulnerable to damage from cellular debris and circulating factors released into the bloodstream after an injury.²⁻⁵ Endotheliopathy in trauma is defined as widespread post-injury disruption of critical endothelial functions including the regulation of microvascular blood flow, barrier integrity, and coagulation. Clinical studies have consistently demonstrated that elevated biomarkers of endothelial injury after severe trauma are important predictors of coagulopathy, multiorgan dysfunction, and death.⁶⁻¹² We have previously used a rodent model of TBI to study the effects of injury on blood pressure control and microvascular function, and reported that TBI impairs both blood pressure control and endothelial-dependent vasodilation in systemic resistance vessels by uncoupling endothelial nitric oxide synthase (eNOS).^{13,14} Recent advances in systems-level screening and analysis have demonstrated profound metabolopathies occur following hemorrhagic shock, TBI, and burn injury, including pronounced alterations in lipid metabolism which would also be expected to impact blood vessel and endothelial functions.¹⁵⁻²⁰ Despite these recent advances, there are few actual studies of systemic vascular endothelial function after shock or trauma, and underlying mechanisms which lead to endotheliopathy in trauma remain elusive. Here, we used our established TBI model to study downstream consequences

injury on a critical modulator of vascular function: the inward rectifier potassium channel Kir2.1.

There are 15 members of the inward rectifier potassium (Kir) channel family. The Kir2 family is strong inward rectifier K⁺ channels, which are activated by external K⁺ and require phosphatidylinositol 4,5-bisphosphate (PIP₂) for activity.²¹ We and others have provided strong evidence that smooth muscle cells (SMCs) and ECs have Kir2.1 channels.²²⁻²⁷ Kir2.1 channel function plays a key role in setting arterial resting membrane potential, myogenic tone development, and cerebral blood flow regulation.^{28,29} We recently demonstrated impaired capillary EC Kir2.1 function in the cortical hemisphere contralateral to a brain injury; but prior studies have not addressed whether this dysfunction extends to blood vessels in the systemic circulation.³⁰ PIP₂ is a minor membrane phospholipid degraded under conditions of oxidative stress or severe inflammation that affect lipid metabolism. Under these conditions, phospholipases (mainly from the A and C families) catalyze membrane phospholipids to form signaling molecules including inositol triphosphate, diacylglycerol, and arachidonic acid (AA). Specifically, PIP₂ is cleaved by phospholipase A₂ (PLA₂) at the sn-2 acyl bond, freeing AA, which is subsequently modified by downstream cyclooxygenases and lipoxygenases into prostanooids and eicosanooids including prostaglandins and leukotrienes.³¹ Disturbed lipid metabolism in severely injured trauma patients is a strong predictor of clinical outcome.³² Altered fatty acid metabolism has been demonstrated in controlled animal models of stroke³³ and tissue injury with hemorrhagic shock, including derangements in mono- and poly-unsaturated fatty acid mobilization and oxidation products.¹⁸ We hypothesized

that severe TBI, even without concomitant shock or hypoxia, would cause significant metabolic responses. In this context, depletion of endothelial PIP₂ in the plasma membrane may impair Kir2.1 channel function and therefore, vascular function. Here, we demonstrate a novel mechanism of altered systemic vascular function after TBI, through PIP₂-dependent impairment of Kir2.1 channel function. The physiological stimulus for vascular Kir2.1 channels is elevation of local K⁺. Impairment of Kir2.1 channel function is significant, as loss of function disrupts control of regional blood flow to metabolically active microvascular beds. Control of PIP₂ levels may provide a therapeutic target to improve vascular function in conditions characterized by altered lipid metabolisms such as TBI and stroke.

Materials and Methods

Animal and Injury Model

Adult male Sprague-Dawley rats (aged 3–4 months; 300–325 g; Charles River, Saint Constant, Quebec, QC, Canada) were randomly assigned to either a fluid percussion TBI surgery or control treatment, as previously described.³⁴ All procedures were approved by the Institutional Animal Care and Use Committee and were performed in accord with the National Research Council's *Guide for the Care and Use of Laboratory Animals*. Animals were anesthetized with inhaled 2%–5% isoflurane prior to TBI or sham surgery. We were unable to conceal group allocations due to obvious postsurgical differences. Male animals were used for all studies due to known sexual dimorphism in response to TBI. All animals received buprenorphine analgesia (subcutaneous; 0.05 mg/kg) while under anesthesia and at 6–12 h after surgery. Briefly, a primary injury was induced by a direct contusion to the brain delivered to the left cerebral hemisphere by a pendulum impacting a fluid-filled chamber connected to the intact dura through a craniotomy.^{29,30} A fluid percussion injury was induced to a target pressure of 4.7 ± 0.1 atm ($n = 36$; ~70 PSI) over a 500 ms period; the pressure was transduced and measured in each surgery. This level of fluid percussion pressure produces a severe injury with approximately 10% mortality. This is consistent with other publications which have defined "severe injuries" as those produced by pressures >2.8 atm.³⁵ This level allows >90% recovery, defined as ability to maintain upright posture, ambulate, and take oral hydration, and produces a highly reproducible outcome of moderate brain injury severity in those surviving animals. Animals that did not recover within 60 min were excluded. These experimental animals have measurable deficits in sensorimotor coordination, along with significant cardiovascular and cerebrovascular effects.^{29,30} Control animals were subjected to scalp incisions but without the percussion injury. At 24 h after recovery from surgery, animals were euthanized using deep pentobarbital anesthesia (intraperitoneal; 0.03 mg/kg) and tissues were collected for experiments.

Sample Preparation and UHPLC-MS Analysis

Plasma was collected and stored at -80°C until analysis. Analyses were performed as previously published.^{36,37} Prior to LC-MS analysis, samples were placed on ice and diluted with 24 volumes of methanol:acetonitrile:water (5:3:2, v:v). Suspensions were vortexed continuously for 30 min at 4°C . Insoluble material was removed by centrifugation at 10 000 g for 10 min at 4°C and supernatants were isolated for metabolomics analysis by

UHPLC-MS. The analytical platform employs a Vanquish UHPLC system (Thermo Fisher Scientific, San Jose, CA) coupled online to a Q Exactive mass spectrometer (Thermo Fisher Scientific, San Jose, CA). Samples were resolved over a Kinetex C18 column, 2.1×150 mm, $1.7 \mu\text{m}$ particle size (Phenomenex, Torrance, CA) equipped with a guard column (SecurityGuardTM Ultracartridge—UHPLC C18 for 2.1 mm ID Columns—AJO-8782—Phenomenex, Torrance, CA) using an aqueous phase (A) of water and 0.1% formic acid and a mobile phase (B) of acetonitrile and 0.1% formic acid for positive ion polarity mode, and an aqueous phase (A) of water:acetonitrile (95:5) with 1 mmol/L ammonium acetate and a mobile phase (B) of acetonitrile:water (95:5) with 1 mmol/L ammonium acetate for negative ion polarity mode. Samples were eluted from the column using either an isocratic elution of 5% B flowed at $250 \mu\text{L}/\text{min}$ and 25°C or a gradient from 5% to 95% B over 1 min, followed by an isocratic hold at 95% B for 2 min, flowed at $400 \mu\text{L}/\text{min}$ and 45°C . The Q Exactive mass spectrometer (Thermo Fisher Scientific, San Jose, CA) was operated independently in positive or negative ion mode, scanning in Full MS mode (2 μscans) from 60 to 900 m/z at 70 000 resolution, with 4 kV spray voltage, 45 sheath gas, 15 auxiliary gas. Calibration was performed prior to analysis using the PierceTM Positive and Negative Ion Calibration Solutions (Thermo Fisher Scientific. Metabolite assignments, isotopologue distributions, and correction for expected natural abundances of deuterium, ¹³C, and ¹⁵N isotopes were performed using MAVEN (Princeton, NJ).³⁸

Electrophysiology

Kir2.1 currents were monitored in freshly isolated ECs and SMCs from third- and fourth-order branches of mesenteric arteries using patch-clamp electrophysiology, as previously described.³⁹ Briefly, mesenteric arteries were harvested and ECs were isolated in 1.5 mL dissociation solution containing (in mmol/L): 134 KCl, 6 KOH, 10 NaOH, 1.1 MgCl₂, 1.8 CaCl₂, 5 EGTA, 10 HEPES (pH 7.3), containing 0.5 mg/mL neutral protease and elastase (0.5 mg/mL; Worthington Biochemical Corp., Lakewood, NJ), for 60 min at 37°C . Collagenase (0.5 mg/mL; Worthington Type I) was added to the dissociation solution for three more minutes. Vessels were then washed in Ca²⁺-free dissociation solution (4°C) for 5–10 min and the solution triturated 10 times through a custom glass Pasteur pipette to release single ECs into the solution. SMCs were isolated in dissociation solution containing 1 mg/mL papain, 0.5 mg/mL dithioerythritol, and 0.5 mg/mL bovine serum albumin for 25 min. Next, 1 mg/mL of collagenase (Worthington Type IV), 0.25 mg/mL elastase, and 0.5 mg/mL Trypsin inhibitor and 100 μM CaCl₂ were exchanged in the solution for 10 min. Electrophysiology was performed in either the conventional or perforated whole-cell configuration. Whole-cell currents were amplified using an Axopatch 200B amplifier (Molecular Devices), filtered at 1 kHz, digitized at 10 kHz, and stored on a computer for offline analysis with Clampfit 10.7 software. Patch pipettes were pulled from borosilicate, microcapillary tubes (1.5-mm O.D., 1.17-mm I.D.; Sutter Instruments, Novato, CA), and fire-polished (resistance ~4–6 M Ω). Cells were voltage-clamped at a holding V_M of -50 mV and equilibrated for 15 min in a bath solution containing (in mmol/L): 134 NaCl, 6 KCl, 1 MgCl₂, 10 glucose, 2 CaCl₂, and 10 HEPES (pH 7.4). For the perforated-patch configuration, pipettes were backfilled with a solution containing (in mmol/L): 10 NaCl, 30 KCl, 110 K⁺-Aspartate, 1 MgCl₂, 10 HEPES (pH 7.2), and 200–250 $\mu\text{g}/\text{mL}$ amphotericin B, added freshly on the day of the experiment. For the conventional whole-cell configuration, the

pipette solution was composed of (in mmol/L): 134 KCl, 6 KOH, 10 NaOH, 1.1 MgCl₂, 1.8 CaCl₂, 5 EGTA, 10 HEPES (pH 7.2). Ba²⁺-sensitive Kir2 currents were quantified by elevating extracellular [K⁺] from 6 to 60 mmol/L via equimolar replacement of NaCl by KCl. A 400-ms voltage-ramp protocol (−140 mV to +40 mV) was applied. All experiments were performed at room temperature (~22°C). Control EC capacitance was 10.7 ± 0.5 pF and TBI EC capacitance was 11.0 ± 0.6 pF. Control SMC capacitance was 11.2 ± 1.0 pF and TBI SMC capacitance was 14.1 ± 0.7 pF.

Oxidation–Reduction Potential (ORP) Measurements

Redox balance (integrated measure of the balance between total oxidants and reductants) was evaluated in plasma samples obtained from control and TBI rats by measuring the oxidation–reduction potential (ORP), or total oxidizing capacity.⁴⁰ Whole blood was collected at the time of euthanasia into an evacuated tube containing heparin and immediately centrifuged (2000 rpm; 4°C). Plasma samples (30 µL) were collected and tested using the RedoxSYS diagnostic platform, consisting of a micro Pt/AgCl combination redox electrode sensor and benchtop analyzer (Aytu Bioscience, Inc., Englewood, CO). Values were recorded in mV after ORP readings were stable for 10 s. The diagnostic platform was calibrated before use and validated in a previous study.¹⁴

PLA₂ Activity Assay

Total PLA₂ activity was measured in plasma samples obtained from control and TBI rats according to manufacturer's instructions (BioVision, San Jose, CA). Briefly, fluorescence readings were taken with a microplate reader every 17 s for 45 min. Activity was calculated from the linear range of the reaction and corrected for volume and time.

Pressure Myography

Pressure myography studies were conducted as previously reported¹³ Immediately after euthanasia, a midline laparotomy was performed and the mesentery was dissected out and placed into cold (4°C) physiological saline solution (PSS) with the following composition (in mmol/L): 119 NaCl, 45 KCl, 24 NaHCO₃, 1 KH₂PO₄, 2.5 CaCl₂, 1 MgCl₂, and 11 glucose (pH 7.4). The mesentery was then pinned out on a dissecting dish and fourth- and fifth-order mesenteric arteries were dissected free from the surrounding adipose and connective tissue. For each experiment, an individual mesenteric artery was cannulated in a pressure myograph (Living Systems Instrumentation, St. Albans, VT) containing oxygenated 20% O₂/5% CO₂ PSS at 37°C. Intraluminal pressure during the experiment was maintained at 80 mm Hg using a pressure servo system, and blood vessel diameters were measured using edge-detection software coupled to a camera (IonOptix, Westwood, MA). Arteries were equilibrated for 10 min, pressurized, and allowed to develop spontaneous myogenic tone over the course of 30 min, defined as >20% constriction after equilibration and pressurization of vessel. Myogenic tone was significantly higher in the TBI group (37 ± 2%; n = 19; P < .05; unpaired t-test) when compared to controls (28 ± 2%; n = 19) as previously reported.¹⁴ The maximal, or passive, diameters obtained in 0-Ca²⁺ PSS with 100 µM diltiazem were not significantly different between control (156 ± 5 µm; n = 19) and TBI groups (161 ± 9 µm; n = 19). The vascular endothelium was considered intact if a dilation of greater than 85% was elicited using the endothelial-dependent vasodilator NS309 (1 µM; Cayman

Chemical Company, Ann Arbor, MI). Arteries that did not develop spontaneous myogenic tone were excluded.

Statistics

Metabolic pathway analysis, PLS-DA, heat mapping, and hierarchical clustering were performed using the MetaboAnalyst 3.0 package (www.metaboanalyst.com).⁴¹ Hierarchical clustering analysis was also performed through the software GENE-E (Broad Institute, Cambridge, MA). GraphPad Prism software (version 6.03; GraphPad Software, La Jolla, CA) was used for X–Y graphing and analysis; values are presented as means ± standard error of the mean. Differences were considered significant if P < .05. Data were tested for normality and a parametric or nonparametric statistical test was subsequently applied. One- or two-way analysis of variance was used for comparisons of multiple group measurements. In a few experimental series, a single control group was used to test multiple hypotheses. To avoid increasing the likelihood of a Type I error, we used the Bonferroni correction to test each individual hypothesis at a significance level determined by $\alpha = 1/m$, where *m* is the number of comparisons.

Results

TBI Impairs Vasoconstriction to Kir2.1 Blockade and Dilates to Elevated Extracellular Potassium

To assess vascular Kir2.1 channel function, the inhibitors BaCl₂ (100 µmol/L; Figure 1A) and ML 133 (20 µmol/L; Figure 1B) were exogenously applied to mesenteric arteries isolated from control and TBI rats. We found that vasoconstrictions to BaCl₂ and ML 133 were both significantly decreased in TBI arteries when compared to controls. Next, a concentration–response curve was performed by exchanging the arteriography chamber buffer with increasing steps of extracellular potassium (K⁺). Dilations to 10 mmol/L extracellular K⁺ were significantly reduced in MAs after TBI (Figure 1C). Concentrations at and greater than 14 mmol/L K⁺ constricted MAs in both groups. Interestingly, constrictions at the maximal concentration of 60 mmol/L K⁺ remained unaltered in TBI animals, suggesting preserved contractility following injury (Figure 1C). These findings suggest that vascular Kir2.1 channel function is crippled following TBI.

Endothelial and Smooth Muscle Kir2.1 Currents Are Significantly Diminished Following TBI and Subsequently Rescued by Exogenous PIP₂

We employed patch-clamp electrophysiology in native EC and SMCs from mesenteric arteries from TBI and control animals. First, we utilized a perforated patch-clamp configuration, in which the cytoplasm remains intact, to measure Kir2.1 currents in freshly isolated cells bathed in a high extracellular [K⁺]_o solution (60 mmol/L), used to amplify the inward component of Kir2.1 current amplitude. Under these conditions, the K⁺ equilibrium potential (E_K) was −23 mV. We found in both EC and SMC barium-sensitive currents were significantly reduced following TBI (Figure 2A and B). One possible explanation for impaired Kir2.1 currents is the loss of the essential cofactor, PIP₂. In support of this, we found the reduction in the Kir2.1 current observed in ECs after trauma was partially restored when the synthetic PIP₂ analog PIP₂ diC8 (10 µmol/L) was included in the intracellular pipette solution. Using conventional whole-cell configurations, we found current densities in the TBI cells treated with PIP₂-diC8 were not significantly different from either the control PIP₂-diC8-treated or naïve control groups (Figure 3).

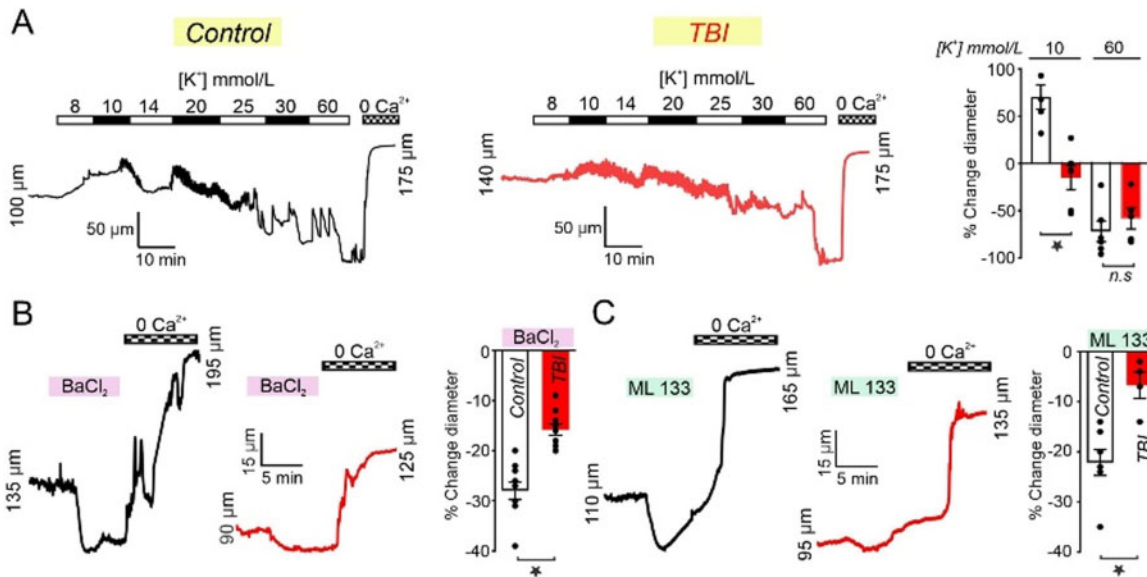


Figure 1. TBI Impairs Vasoconstrictions to the Kir2.1 Channel Blockers BaCl₂ and ML 133 and Dilations to Extracellular K⁺ in Mesenteric Arteries. (A) Raising extracellular K⁺ from 6 to 8 mmol/L caused an immediate 43 ± 13% (n = 4) vasodilation and a subsequent peak dilation at 10 mmol/L K⁺ (62 ± 13%; n = 4) in control MBAs pressurized to 80 mm Hg. As the concentration of extracellular K⁺ continued to increase from 14 to 60 mmol/L, constrictions were observed in both control and TBI arteries. In MBAs from TBI animals responses to 10 mmol/L K⁺ were significantly diminished when compared to controls (-15 ± 13%; n = 6; P < 0.05; unpaired t-test). (B) BaCl₂ (100 μmol/L)-induced constrictions were significantly diminished in TBI arteries (-16 ± 1.1%; n = 10) when compared to controls (-28 ± 1.7%; n = 12; P < 0.0001; unpaired t-test). (C) Constrictions to ML 133 (20 μmol/L) were significantly reduced in TBI arteries (-6.8 ± 2.6%; n = 4) when compared to controls (-22 ± 2.6%; n = 7; P = 0.0091; unpaired t-test).

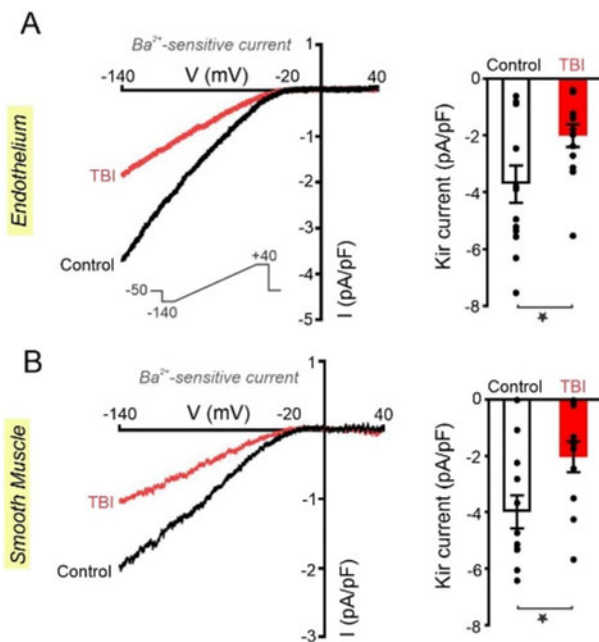


Figure 2. TBI Diminishes Kir2.1 Currents in Mesenteric Endothelial and SMCs. Whole-cell current was measured in freshly isolated endothelial and SMCs in a high extracellular K⁺ solution (60 mmol/L) using a voltage ramp protocol (-140 to +40 mV) and perforated whole-cell patch-clamp configuration, in the absence and presence of BaCl₂ (100 μmol/L) (A) Representative whole-cell recordings of Ba²⁺-sensitive currents in ECs from control (n = 13) and TBI (n = 13) rats. Kir2.1 current density at -140 mV is significantly diminished in ECs from TBI rats when compared to controls (-2.0 ± 0.4 pA/pF, n = 13, vs -3.7 ± 0.7 pA/pF, n = 13, P = 0.03, unpaired t-test). (B) Representative whole-cell recording of Ba²⁺-sensitive currents in SMCs from control (n = 12) and TBI (n = 11) animals. Similarly, SMC Kir2.1 current density at -140 mV is significantly diminished after TBI when compared to controls (-1.01 ± 0.3 pA/pF, n = 11, vs -1.9 ± 0.3 pA/pF, n = 12, P = 0.02, unpaired t-test; Figure 2B).

TBI Elevates Hydrogen Peroxide-Derived Oxidative Stress and Phospholipase A₂ Activity

We previously showed uncoupling of eNOS in systemic arteries after TBI which would be expected to increase vascular hydrogen peroxide (H₂O₂) levels.¹⁴ Oxidative stress is known to activate PLA₂ and contribute to the deranged lipidome observed after TBI.^{42–46} We therefore sought to measure global oxidant levels in plasma, and the response of mesenteric arteries to catalase, after TBI. We measured oxidation–reduction potential in plasma before and after the addition of catalase (500 U/mL). The oxidation–reduction potential after TBI was significantly higher compared to controls and was reduced to a level equal to controls by catalase (Figure 4A). This indicates that the overall state of oxidation is elevated in TBI plasma, and that H₂O₂ is the reactive oxidant species responsible for this elevation. In pressurized mesenteric arteries, constrictions to catalase (500 U/mL) were significantly increased following TBI (Figure 4B). In addition, total PLA₂ activity (mU/mL) was significantly increased in plasma from injured animals when compared to controls (Figure 4C). These findings support a model of H₂O₂-derived PLA₂ activity which would be expected to alter lipid metabolism and PIP₂ levels after TBI.

TBI Disrupts Lipid Metabolism Causing Accumulation of PIP₂ Degradation Products

A high-throughput, semi-targeted metabolomics approach was applied to evaluate the metabolome of rats in our model of TBI, which has been shown to induce endothelial dysfunction in remote blood vessels from the mesenteric circulation.¹⁴ A correlation matrix and heat map for the top 50 metabolites with the lowest P-values studied in plasma from control and TBI rats are shown (Figure 5A and B). Individual metabolites may be seen in Supplementary Table S1. Partial least squares discriminant analysis (PLS-DA) of control and TBI groups of metabolite

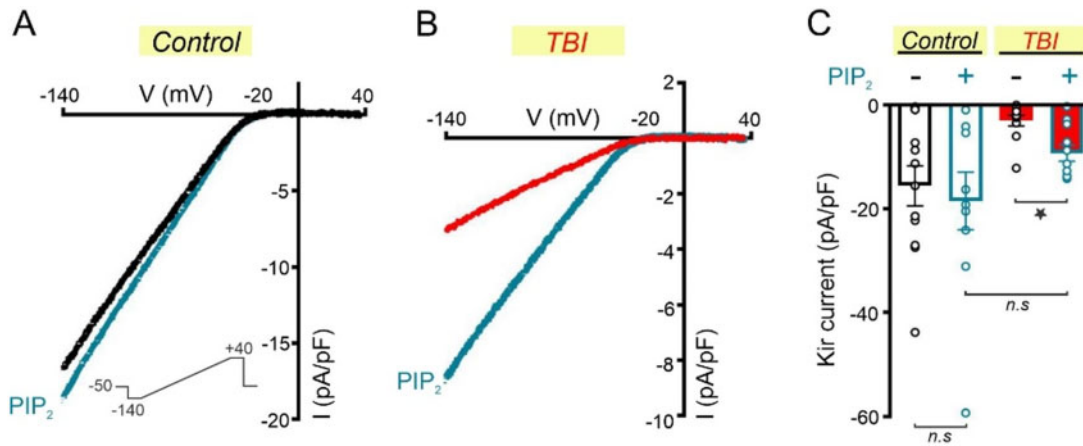


Figure 3. The PIP₂ Analog PIP₂ diC8 Rescues Endothelial Kir2.1 Currents after TBI. Whole-cell currents were measured in freshly isolated endothelial and SMCs in a high extracellular K⁺ solution (60 mmol/L) using a voltage ramp protocol (−140 to +40 mV) and conventional whole-cell patch-clamp configuration, in the absence and presence of BaCl₂ (100 μmol/L). The PIP₂ analog PIP₂ diC8 (10 μmol/L) was included in the patch pipette. (A) Representative whole-cell recording of Ba²⁺-sensitive currents from control and TBI MAs in the absence or presence of PIP₂-diC8 (10 μmol/L). (B) Summary data of peak inward current (−140) in ECs dialyzed with or without PIP₂ from control or TBI groups. Kir2.1 current density was significantly diminished after TBI in MA ECs when compared to control ECs without PIP₂ (−2.9 ± 1.0 pA/pF, n = 11 vs −15.7 ± 3.8 pA/pF, n = 12; P < 0.0062; unpaired t-test). No difference was observed in Kir2.1 current density (−140 mV) in the presence or absence of PIP₂ in ECs from control MAs (−18.5 ± 5.5 pA/pF, n = 10, vs −15.7 ± 3.8 pA/pF, n = 12; n.s.; unpaired t-test). Kir2.1 current density was significantly increased in TBI ECs in the presence of PIP₂ when compared to TBI ECs without PIP₂ (−8.6 ± 1.6 pA/pF, n = 12, vs −2.9 ± 1.0 pA/pF, n = 11; P < 0.0078; unpaired t-test). There was no significant difference in Kir2.1 current density in control and TBI ECs in the presence of PIP₂, implying a rescue of functional Kir2.1 channels and a return to control-level current densities in the ECs from TBI MAs.

levels in each biological replicate showed that the trauma and control samples clustered in distinct metabolic phenotypes (Figure 5C). Fold-change comparisons between TBI and control animals are shown as graphs of lipid metabolites. Of particular interest, we noted that TBI produced profound alterations in certain lipids, including increases in circulating eicosatetraenoic acid and AA, which can derive from PIP₂ degradation. Downstream products of AA metabolism were also altered, including prostanoids, eicosanoids, and leukotrienes (Figure 5D).

Discussion

Here, we used a well-characterized model of TBI, known to produce systemic effects of increased blood pressure and impaired endothelial-dependent vasodilatory function, to study the role of Kir2.1 in the endotheliopathy of trauma. This study has three relevant findings. First, TBI cripples systemic vascular Kir2.1 channel function, evident in both single cell (EC and SMC) and intact vascular preparations. This has important clinical implications, as vascular Kir2.1 signaling modulates blood flow.³⁹ Second, we provide a plausible mechanism for trauma-induced endothelial dysfunction; an increase in circulating and cellular H₂O₂-derived oxidative stress which causes an increase in PLA₂ activity that would be expected to degrade PIP₂ and thereby altering Kir2.1 channel function. Third, the fact that Kir2.1 channel function in isolated cells was rescued with PIP₂ suggests a potential therapeutic strategy to improve endothelial function, providing a rationale for future experiments that will determine the efficacy of PIP₂ treatment in trauma models. Additionally, we demonstrate that an isolated TBI, even without shock or hypoxia, produces a profound lipidopathy and an increase in H₂O₂ levels in both plasma and small blood vessels. A metabolomics screen was conducted to determine metabolic alterations in our TBI model which might impact vascular functions. This probe identified dysregulation of lipid metabolism pathways, including alteration of arachidonate pathways and

phospholipid synthesis, and fatty acid mobilization/oxidation which are hallmarks of inflammation. Increases in H₂O₂-derived oxidative stress and phospholipase activity in plasma were consistent with upregulation of lipid metabolism.^{19,42,45,47} We focused on PIP₂, a specific membrane phospholipid and key modulator of Kir2.1, the molecular feature that regulates myogenic tone and electrical conduction through the vascular endothelium.^{28,48–51}

Endotheliopathy in Trauma

Recent studies have reported that biomarkers of endothelial dysfunction correlate with injury severity and adverse outcomes including coagulopathy and multiorgan dysfunction in trauma patients. Biomarkers reflecting endothelial damage or activation by cytokines include syndecan-1, thrombomodulin, and E-selectin.^{7,8,10,52} These biosignatures are elevated after isolated TBI and/or multisystem injury, in adults and children, and in both the prehospital setting and after resuscitation. These reports have suggested the existence of a pervasive “endotheliopathy of trauma” which complicates recovery and prevents optimizing the management of uncontrolled hemorrhage and coagulopathy; yet few studies have actually evaluated EC or vascular function directly after trauma. Animal models of trauma provide the opportunity to directly study blood vessels to further elucidate the cellular mechanisms of endothelial injury. We previously described abnormal blood pressure control and impaired endothelial-dependent vasodilation in blood vessels harvested from the mesenteric circulation, remote from the site of TBI, but, to our knowledge, the function of vascular Kir2.1 channels in trauma has not been previously assessed.^{13,14} Here, we provide a novel mechanism for endothelial dysfunction, showing that Kir2.1 function in pressurized arteries and isolated vascular cells is significantly diminished; thus, providing a novel model to elucidate dysfunction in the endotheliopathy of trauma.

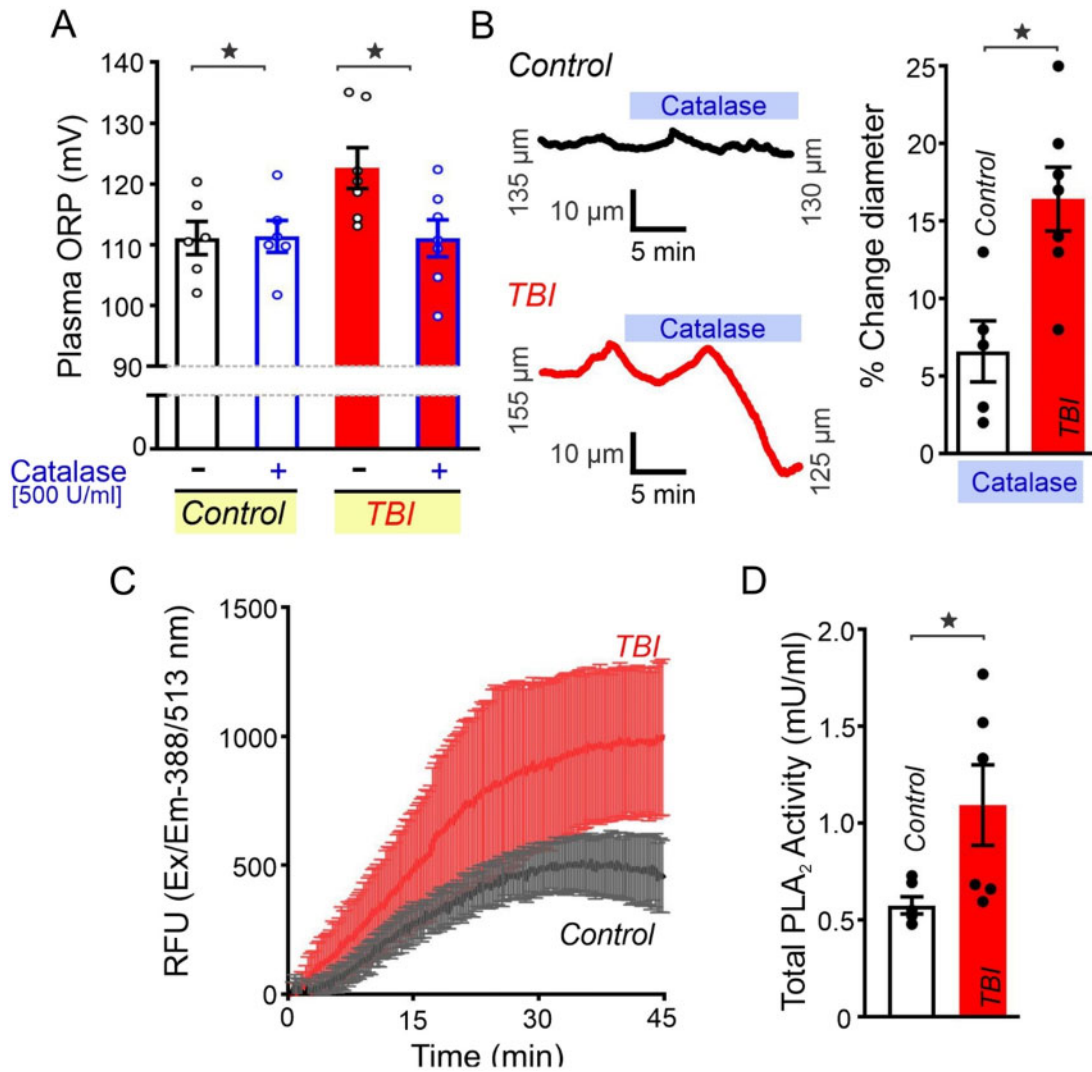


Figure 4. H₂O₂ Levels and PLA₂ Activity Are Significantly Increased in Mesenteric Arteries and Plasma from TBI rats. (A) Oxidative reduction potential (ORP) measurements using the Redoxsys platform were conducted in paired plasma samples from control and TBI rats with and without the addition of catalase (500 U/mL). Plasma ORP was unchanged in control samples before and after the addition of catalase (500 U/mL) (111.1 ± 2.7 mV vs 111.4 ± 2.6 mV, n = 6; n.s.; paired t-test). ORP in TBI plasma samples was significantly decreased to control values after the addition of catalase (500 U/mL) (122.6 ± 3.6 mV vs 111.1 ± 3.0 mV, n = 7, P = 0.0017, paired t-test). (B) Constrictions to catalase (500 U/mL) were significantly increased in mesenteric arteries from TBI rats when compared to controls (16.4 ± 2.01%, n = 7 vs 6.6 ± 2.0%, n = 5, P = 0.0077; unpaired t-test). (C) Averaged time course of PLA₂ activity in control and TBI plasma samples. (D) Total PLA₂ activity is significantly increased in plasma from TBI rats when compared to controls (1.095 ± 0.21 mU/mL, n = 6 vs 0.576 ± 0.05 mU/mL, n = 6, P = 0.0352; unpaired t-test).

Kir2.1 Channel Dysfunction and PIP₂ Regulation

The Kir2.1 channel is the molecular cornerstone responsible for dynamic regulation of blood flow in the brain and other excitable tissues, and the membrane phospholipid PIP₂ is required for channel function.²¹ Kir2.1 channels are exquisitely sensitive to changes of extracellular K⁺, which acts as a potent vasodilator. In the brain, capillary endothelial Kir2.1 channels play a critical role in the dynamic regulation of regional perfusion, by conducting a spreading hyperpolarizing signal in response to locally elevated extracellular K⁺ released during neural activity, and thereby directing blood flow.²⁸ We demonstrated that the electrical response of brain capillary endothelial Kir2.1 and its ability to direct blood flow depends on PIP₂ levels.⁵¹ Cerebral ischemia leads to a loss of functional Kir2.1 channels in parenchymal arteriole smooth muscle, impairing neurovascular coupling.⁵³ In addition, others have investigated the effect of

fluid percussion injury on ATP-sensitive potassium channels and calcium-activated potassium channels in the cerebral vasculature.^{54–56} Our current study is novel as we elucidate the effects of TBI on EC inward rectifier potassium channels in a remote, systemic tissue bed. We recently found that a TBI results in impaired Kir2.1 channel function in capillary ECs from the opposite side of the brain, and we hypothesized that this dysfunction may be widespread and not limited to cerebral endothelium. Endothelial Kir2.1 channels are also important in mesenteric resistance arteries, boosting vasodilatory signals through endothelial-derived hyperpolarizing pathways.⁴⁸ Our results support a model by which systemic oxidative stress, involving H₂O₂, acts via PLA₂ to disrupt Kir2.1 function (Figure 6). Our model provides a plausible mechanism by which the metabolic stress of trauma leads to systemic endothelial dysfunction, based on the known link between H₂O₂ and PLA₂ activation.^{42,47,57,58}

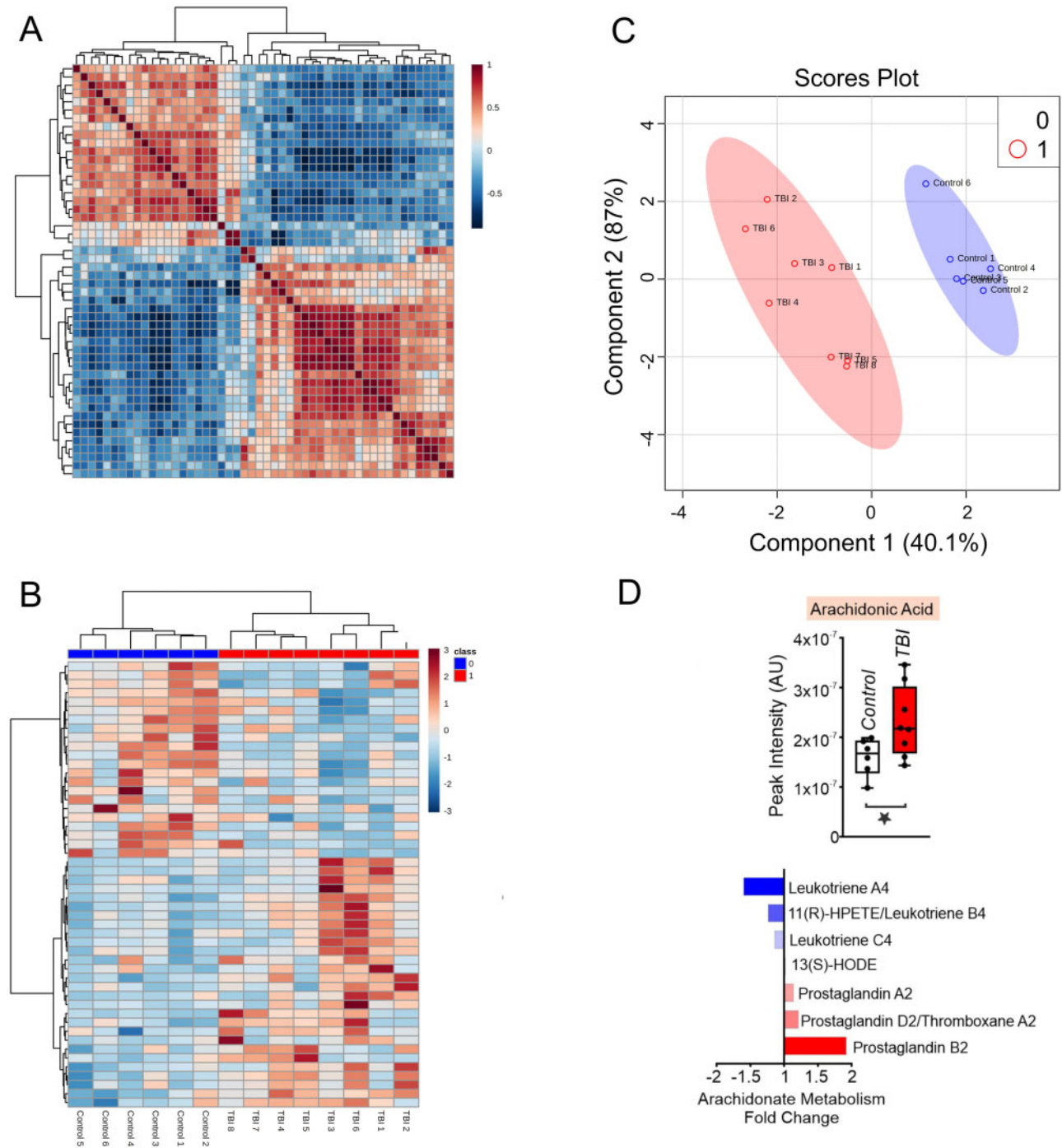


Figure 5. TBI Causes Accumulation of PIP₂ Degradation Products and a Profound Lipidopathy. (A) Correlation matrix (distance measure: Pearson *r*) of the top 50 metabolites sorted by lowest *P*-value and (B) a heat map (distance measure: Euclidean; clustering algorithm: Ward) of the same dataset. (C) Scores plot with Component 1 on the x-axis contributes to 40.1% of the total variance. Component 2 on the y-axis contributes to 87% of the total variance. (D) Circulating AA (eicosatetraenoic acid) is significantly increased in plasma from TBI rats when compared to controls (2.3×10^7 median AU, *n*=8 vs 1.6×10^7 median AU, *n*=6, *P*<0.05). Arachidonate metabolism pathway fold changes after TBI.

Deranged Lipid Metabolism, H₂O₂, and PLA₂ after TBI

Providing further support for our model, our metabolomics screen demonstrated that lipid metabolism homeostasis is significantly deranged as early as 1 day after TBI. These findings correlate with prior reports on TBI during the subacute and chronic phases suggesting that disturbed lipid metabolism is a strong predictor of clinical outcome.^{18,32} With the aid of mass

spectrometry-based lipidomics, they provided quantitative characterization of lipid peroxidation products after TBI and acknowledge PLA₂ as an important mediator in the hydrolysis of peroxidized phospholipids.⁵⁸ The polyunsaturated fatty acid (PUFA) component of membrane phospholipids are often targets for peroxidation, broadly defined as the process of inserting a hydroperoxy group into a lipid. Peroxidation increases the

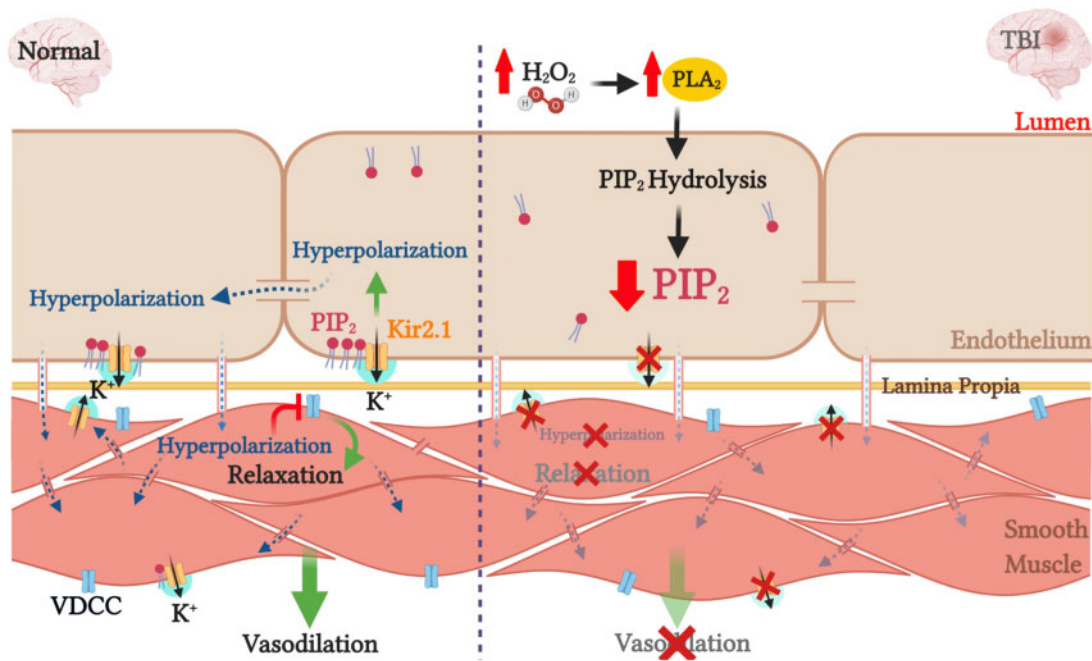


Figure 6. Schematic Overview. As PIP₂ is required to stabilize Kir2.1 channel activity, and H₂O₂ drives down PIP₂ levels, we hypothesized that TBI results in impaired Kir2.1 channel function in MAs. We demonstrated that 24 h following TBI an increase in circulating and cellular H₂O₂-derived oxidative stress causes an increase in PLA₂ activity which degrades PIP₂ in the cell membrane, thereby impairing Kir2.1 channel function and subsequent hyperpolarization/vessel dilation.

rates of hydrolysis by phospholipases. The extent of lipid peroxidation after severe TBI correlates with injury severity and mortality.⁵⁸ Rodent models have also provided insight into specific changes in lipid metabolism induced by trauma. Major changes in free fatty acids, including docosahexaenoic, stearic, oleic, and AAs, were sustained from 4 to 35 days after injury in a rat.⁵⁹ In addition, significant upregulation in PUFAs and PUFA-containing diacylglycerols and changes in membrane phospholipids including sphingolipids have been observed at 1 week after injury.¹⁷ Lipidomic analyses in mouse model of TBI identified injury-specific phospholipid changes that persisted as long as 3 months after trauma induction.¹⁵ Our findings showed that not only lipid metabolites were altered after TBI, but also plasma H₂O₂ and PLA₂ activity were significantly increased in these animals. Specific metabolites of PLA₂-dependent PIP₂ degradation products, such as AA and its downstream metabolites, were effectively detected in our model of TBI. In this context, increased oxidative stress has been described after severe trauma and in TBI in particular.⁶⁰

Conclusions

Collectively, our results support a novel mechanism to explain endotheliopathy in trauma, through diminished Kir2.1 responses which can be rescued by PIP₂. These findings may be generalizable to other pathological conditions characterized by altered lipid metabolism pathways and reductions in PIP₂ levels, and suggest PIP₂ may be a potential therapeutic target to improve endothelial function in conditions characterized by altered lipid metabolism such as brain trauma and stroke. Further investigations are warranted to determine the relevant time course along with the potential for sexual dimorphism in Kir2.1 channel function after TBI. In addition, experiments to explore the effect of plasma H₂O₂, sPLA₂, and altered lipid metabolism on vascular Kir2.1 function in which animals are pretreated

with PEG-Catalase or sPLA₂ inhibitors prior to surgery would provide additional evidence to support our model and could inform future therapeutic strategies.

Supplementary Material

Supplementary material is available at the APS Function online.

Authors' Contributions

A.M.S. designed experiments, acquired, and analyzed data, wrote the initial draft, and edited all subsequent drafts of the manuscript. N.V. assisted with experimental design and participated in all stages of critical revisions. A.D.B. acquired and analyzed electrophysiology data. A.D. and T.M. acquired and analyzed mass spectrometry data. M.S. contributed to data representation and in critical revisions of the manuscript. O.F.H. participated in critical revisions of the manuscript. M.T.N. and K.F. directed the study and edited the manuscript. All authors reviewed the manuscript, contributed to critical revisions, and approved its submission.

Funding

This work was supported by the American Heart Association (17POST33650030 and 20CDA35310097), the Department of Defense Henry M. Jackson Foundation for the Advancement of Military Medicine (HU001-18-2-0016), EC Horizon 2020 Foundation Leducq, and the National Institutes of Health (P20GM135007, R01GM123010, UM1 HL120877, R35HL140027, and R01NS110656), and the Totman Medical Research Trust.

Conflict of interest statement

O.F.H. and M.T.N. are inventors of patent number 62/823,378 “Methods to promote cerebral blood flow in the brain” which was submitted on 25 March 2019. M.T.N. holds the position of Executive Editor for Function and is blinded from reviewing or making decisions for the manuscript.

References

- Heron M. Deaths: leading causes for 2015. *Natl Vital Stat Rep* 2017;66(5):1–76.
- Abrams ST, Zhang N, Manson J, et al. Circulating histones are mediators of trauma-associated lung injury. *Am J Respir Crit Care Med* 2013;187(2):160–169.
- McKee CA, Lukens JR. Emerging roles for the immune system in traumatic brain injury. *Front Immunol* 2016;7:556.
- Xu J, Zhang X, Pelayo R, et al. Extracellular histones are major mediators of death in sepsis. *Nat Med* 2009;15(11):1318–1321.
- Fattahi F, Grailer JJ, Jajou L, Zetoune FS, Andjelkovic AV, Ward PA. Organ distribution of histones after intravenous infusion of FITC histones or after sepsis. *Immunol Res* 2015;61(3):177–186.
- Zeerleder S, Stephan F, Emonts M, et al. Circulating nucleosomes and severity of illness in children suffering from meningococcal sepsis treated with protein C. *Crit Care Med* 2012;40(12):3224–3229.
- Woodcock T, Morganti-Kossmann MC. The role of markers of inflammation in traumatic brain injury. *Front Neurol* 2013;4:18. doi: 10.3389/fneur.2013.00018.
- Gonzalez Rodriguez E, Cardenas JC, Cox CS, et al. Traumatic brain injury is associated with increased syndecan-1 shedding in severely injured patients. *Scand J Trauma Resusc Emerg Med* 2018;26(1):102.
- Jullienne A, Obenaus A, Ichkova A, Savona-Baron C, Pearce WJ, Badaut J. Chronic cerebrovascular dysfunction after traumatic brain injury. *J Neurosci Res*. 2016;94(7):609–622.
- Russell RT, Christiaans SC, Nice TR, et al. Histone-complexed DNA fragments levels are associated with coagulopathy, endothelial cell damage, and increased mortality after severe pediatric trauma. *Shock* 2018;49(1):44–52.
- Alhamdi Y, Zi M, Abrams ST, et al. Circulating histone concentrations differentially affect the predominance of left or right ventricular dysfunction in critical illness. *Crit Care Med* 2016;44(5):e278–e288.
- Ekaney ML, Otto GP, Sossdorf M, et al. Impact of plasma histones in human sepsis and their contribution to cellular injury and inflammation. *Crit Care* 2014;18(5):543.
- Larson BE, Stockwell DW, Boas S, et al. Cardiac reactive oxygen species after traumatic brain injury. *J Surg Res* 2012;173(2):e73–e81.
- Villalba N, Sackheim AM, Nunez IA, et al. Traumatic brain injury causes endothelial dysfunction in the systemic microcirculation through arginase-1-dependent uncoupling of endothelial nitric oxide synthase. *J Neurotrauma* 2017;34(1):192–203.
- Abdullah L, Evans JE, Ferguson S, et al. Lipidomic analyses identify injury-specific phospholipid changes 3 mo after traumatic brain injury. *FASEB J* 2014;28(12):5311–5321.
- Emmerich T, Abdullah L, Crynen G, et al. Plasma lipidomic profiling in a military population of mild traumatic brain injury and post-traumatic stress disorder with apolipoprotein E varepsilon4-dependent effect. *J Neurotrauma* 2016;33(14):1331–1348.
- Hogan SR, Phan JH, Alvarado-Velez M, et al. Discovery of lipidome alterations following traumatic brain injury via high-resolution metabolomics. *J Proteome Res* 2018;17(6):2131–2143.
- Slaughter AL, Nunns GR, D’Alessandro A, et al. The metabolopathy of tissue injury, hemorrhagic shock, and resuscitation in a rat model. *Shock* 2018;49(5):580–590.
- Horton JW. Free radicals and lipid peroxidation mediated injury in burn trauma: the role of antioxidant therapy. *Toxicology* 2003;189(1–2):75–88.
- Kay AD, Day SP, Kerr M, Nicoll JA, Packard CJ, Caslake MJ. Remodeling of cerebrospinal fluid lipoprotein particles after human traumatic brain injury. *J Neurotrauma* 2003;20(8):717–723.
- Harraz OF, Hill-Eubanks D, Nelson MT. PIP2: a critical regulator of vascular ion channels hiding in plain sight. *Proc Natl Acad Sci USA* 2020;117(34):20378–20389.
- Smith PD, Brett SE, Luykenaar KD, et al. KIR channels function as electrical amplifiers in rat vascular smooth muscle. *J Physiol* 2008;586(4):1147–1160.
- Crane GJ, Walker SD, Dora KA, Garland CJ. Evidence for a differential cellular distribution of inward rectifier K channels in the rat isolated mesenteric artery. *J Vasc Res* 2003;40(2):159–168.
- Climent B, Zsiros E, Stankevicius E, et al. Intact rat superior mesenteric artery endothelium is an electrical syncytium and expresses strong inward rectifier K+ conductance. *Biochem Biophys Res Commun* 2011;410(3):501–507.
- Marrelli SP, Johnson TD, Khorovets A, Childres WF, Bryan RM Jr. Altered function of inward rectifier potassium channels in cerebrovascular smooth muscle after ischemia/reperfusion. *Stroke* 1998;29(7):1469–1474.
- Bradley KK, Jaggard JH, Bonev AD, et al. Kir2.1 encodes the inward rectifier potassium channel in rat arterial smooth muscle cells. *J Physiol* 1999;515(Pt 3):639–651.
- Zaritsky JJ, Eckman DM, Wellman GC, Nelson MT, Schwarz TL. Targeted disruption of Kir2.1 and Kir2.2 genes reveals the essential role of the inwardly rectifying K(+) current in K(+)-mediated vasodilation. *Circ Res* 2000;87(2):160–166.
- Longden TA, Nelson MT. Vascular inward rectifier K+ channels as external K+ sensors in the control of cerebral blood flow. *Microcirculation* 2015;22(3):183–196.
- Quayle JM, Nelson MT, Standen NB. ATP-sensitive and inwardly rectifying potassium channels in smooth muscle. *Physiol Rev* 1997;77(4):1165–1232.
- Mughal A, Sackheim AM, Sancho M, et al. Impaired capillary-to-arteriolar electrical signaling after traumatic brain injury. *J Cereb Blood Flow Metab* 2020;271678X20962594. doi:10.1177/0271678X20962594.
- Filkin SY, Lipkin AV, Fedorov AN. Phospholipase superfamily: structure, functions, and biotechnological applications. *Biochemistry (Moscow)* 2020;85(Suppl 1):S177–S195.
- Cohen MJ, Serkova NJ, Wiener-Kronish J, Pittet JF, Niemann CU. 1H-NMR-based metabolic signatures of clinical outcomes in trauma patients—beyond lactate and base deficit. *J Trauma* 2010;69(1):31–40.
- Haley MJ, White CS, Roberts D, et al. Stroke induces prolonged changes in lipid metabolism, the liver and body composition in mice. *Transl Stroke Res* 2020;11(4):837–850.
- Villalba N, Sonkusare SK, Longden TA, et al. Traumatic brain injury disrupts cerebrovascular tone through endothelial inducible nitric oxide synthase expression and nitric oxide gain of function. *J Am Heart Assoc* 2014;3(6):e001474.

35. Kabadi SV, Hilton GD, Stoica BA, Zapple DN, Faden AI. Fluid-percussion-induced traumatic brain injury model in rats. *Nat Protoc* 2010;5(9):1552–1563.
36. Nemkov T, Hansen KC, D'Alessandro A. A three-minute method for high-throughput quantitative metabolomics and quantitative tracing experiments of central carbon and nitrogen pathways. *Rapid Commun Mass Spectrom* 2017;31(8):663–673.
37. Nemkov T, Reisz JA, Gehrke S, Hansen KC, D'Alessandro A. High-throughput metabolomics: isocratic and gradient mass spectrometry-based methods. *Methods Mol Biol* 2019;1978:13–26. doi:10.1007/978-1-4939-9236-2_2.
38. Clasquin MF, Melamud E, Rabinowitz JD. LC-MS data processing with MAVEN: a metabolomic analysis and visualization engine. *Curr Protoc Bioinformatics* 2012;Chapter 14:Unit14 11. doi: 10.1002/0471250953.bi1411s37.
39. Sonkusare SK, Dalsgaard T, Bonev AD, Nelson MT. Inward rectifier potassium (Kir2.1) channels as end-stage boosters of endothelium-dependent vasodilators. *J Physiol* 2016;594(12):3271–3285. doi: 10.1113/JP271652.
40. Polson D, Villalba N, Freeman K. Optimization of a diagnostic platform for oxidation-reduction potential (ORP) measurement in human plasma. *Redox Rep* 2018;23(1):125–129.
41. Xia J, Sinelnikov IV, Han B, Wishart DS. MetaboAnalyst 3.0—making metabolomics more meaningful. *Nucleic Acids Res* 2015;43(W1):W251–W257.
42. Goldman R, Ferber E, Zort U. Reactive oxygen species are involved in the activation of cellular phospholipase A2. *FEBS Lett* 1992;309(2):190–192.
43. Chen H, Man RYK, Leung SWS. PPAR- α agonists acutely inhibit Ca²⁺-independent PLA2 to reduce H2O2-induced contractions in aortae of spontaneously hypertensive rats. *Am J Physiol Heart Circ Physiol* 2018;314(3):H681–H691.
44. Colston JT, de la Rosa SD, Strader JR, Anderson MA, Freeman GL. H2O2 activates Nox4 through PLA2-dependent arachidonic acid production in adult cardiac fibroblasts. *FEBS Lett* 2005;579(11):2533–2540.
45. Ginsburg I, Mitra RS, Gibbs DF, Varani J, Kohen R. Killing of endothelial cells and release of arachidonic acid. Synergistic effects among hydrogen peroxide, membrane-damaging agents, cationic substances, and proteinases and their modulation by inhibitors. *Inflammation* 1993;17(3):295–319.
46. Dan P, Nitzan DW, Dagan A, Ginsburg I, Yedgar S. H2O2 renders cells accessible to lysis by exogenous phospholipase A2: a novel mechanism for cell damage in inflammatory processes. *FEBS Lett* 1996;383(1–2):75–78.
47. Boyer CS, Bannenberg GL, Neve EP, Ryrfeldt A, Moldeus. Evidence for the activation of the signal-responsive phospholipase A2 by exogenous hydrogen peroxide. *Biochem Pharmacol*. 1995;50(6):753–761.
48. Ahn SJ, Fancher IS, Bian JT, et al. Inwardly rectifying K(+) channels are major contributors to flow-induced vasodilatation in resistance arteries. *J Physiol* 2017;595(7):2339–2364.
49. Chrissobolis S, Sobey CG. Inwardly rectifying potassium channels in the regulation of vascular tone. *Curr Drug Targets* 2003;4(4):281–289.
50. Hansen SB. Lipid agonism: the PIP2 paradigm of ligand-gated ion channels. *Biochim Biophys Acta* 2015;1851(5):620–628.
51. Harraz OF, Longden TA, Dabertrand F, Hill-Eubanks D, Nelson MT. Endothelial GqPCR activity controls capillary electrical signaling and brain blood flow through PIP2 depletion. *Proc Natl Acad Sci USA* 2018;115(15):E3569–E3577.
52. Wu F, Chipman A, Pati S, Miyasawa B, Corash L, Kozar RA. Resuscitative strategies to modulate the endotheliopathy of trauma: from cell to patient. *Shock* 2019. doi: 10.1097/SHK.0000000000001378.
53. Povlsen GK, Longden TA, Bonev AD, Hill-Eubanks DC, Nelson MT. Uncoupling of neurovascular communication after transient global cerebral ischemia is caused by impaired parenchymal smooth muscle Kir channel function. *J Cereb Blood Flow Metab* 2016;36(7):1195–1201. doi: 10.1177/0271678X16638350.
54. Armstead WM. Role of impaired cAMP and calcium-sensitive K⁺ channel function in altered cerebral hemodynamics following brain injury. *Brain Res* 1997;768(1–2):177–184.
55. Armstead WM. Brain injury impairs ATP-sensitive K⁺ channel function in piglet cerebral arteries. *Stroke* 1997;28(11):2273–2279; discussion 2280.
56. Armstead WM. ATP-dependent K⁺ channel activation reduces loss of opioid dilation after brain injury. *Am J Physiol* 1998;274(5):H1674–H1683.
57. Phillis JW, O'Regan MH. The role of phospholipases, cyclooxygenases, and lipoxygenases in cerebral ischemic/traumatic injuries. *Crit Rev Neurobiol* 2003;15(1):61–90.
58. Anthony-muthu TS, Kenny EM, Bayir H. Therapies targeting lipid peroxidation in traumatic brain injury. *Brain Res* 2016; 1640(Pt A):57–76. doi: 10.1016/j.brainres.2016.02.006.
59. Homayoun, Rodriguez de Turco EB, Parkins NE, et al. Delayed phospholipid degradation in rat brain after traumatic brain injury. *J Neurochem* 1997;69(1):199–205.
60. Parihar A, Parihar MS, Milner S, Bhat S. Oxidative stress and anti-oxidative mobilization in burn injury. *Burns* 2008;34(1):6–17.